Magn Reson Med Sci 2018; 17; 132–137
doi:10.2463/mrms.mp.2017-0088
Published Online: September 29, 2017

MAJOR PAPER

Appearance of the Organum Vasculosum of the Lamina Terminalis on Contrast-enhanced MR Imaging

Shinji Naganawa[1*], Toshiaki Taoka[1], Hisashi Kawai[1], Masahiro Yamazaki[1], and Kojiro Suzuki[1,2]

Purpose: Circumventricular organs (CVOs) lack a blood brain barrier and are also called "brain windows". Among CVOs, the organum vasculosum of the lamina terminalis (OVLT) is an osmotic regulator involved in the release of vasopressin. In a previous study of healthy subjects, it was reported that contrast enhancement in the OVLT can be recognized in only 34% of 3 Tesla thin slice contrast-enhanced T_1-weighted images. The purpose of this study was to evaluate the leakage of gadolinium contrast from the OVLT in healthy subjects using heavily T_2-weighted three dimensional-fluid attenuated inversion recovery (3D-FLAIR) (HF) imaging.

Methods: Eight healthy male subjects were included in this study. A standard dose (0.1 mmol/kg) of gadoteridol was intravenously administered. Magnetic resonance cisternography (MRC) and HF were obtained before and 0.5, 1.5, 3, 4.5 and 6 h after the injection. Enhancement of the OVLT including the surrounding cerebral spinal fluid (CSF) was measured by manually drawing a rectangular ROI centered on the OVLT. The ROI was copied to the HF image and the signal intensity was measured. The signal intensity ratio (SIR) was obtained by dividing the signal intensity value of the OVLT ROI by that of the midbrain.

Results: The differences between the mean SIR at pre-contrast and those at 0.5, 1.5, 3, 4.5, and 6 h were significant ($P < 0.05$). The mean SIR at 0.5 h was higher than those at all other time points ($P < 0.05$).

Conclusion: Using HF imaging, enhancement around the OVLT was observed in all subjects at 0.5 h after intravenous administration of single dose gadoteridol.

Keywords: *magnetic resonance imaging, three dimensional imaging, organum vasculosum of lamina terminalis*

Introduction

Circumventricular organs (CVOs) lack a blood brain barrier and are also called "brain windows". There is some controversy regarding the actual number of CVOs. One definition describes the presence of seven CVOs.[1] The median eminence (ME), neurohypophysis (NH), subforniceal organ (SFO), organum vasculosum of the lamina terminalis (OVLT), area postrema (AP), subcommissural organ (SCO), and the pineal gland (PG) are cited as CVOs.[1–3] They are classified as secretory periventricular organs and sensory periventricular organs. The AP, SFO, and OVLT are sensory organs,[4] and the others, except the SCO, are secretory organs. Secretory CVOs have been shown to be enhanced consistently on T_1-weighted images, while sensory CVOs were less enhanced.[5] The SCO is not highly permeable and does not have fenestrated capillaries.[2] The specific function of the SCO is still unclear.[1] Recently it was reported that tuber cinereum showed unequivocal enhancement on T_1-weighted images in all subjects, and tuber cinereum is also speculated as one of CVOs.[5]

CVOs are located around the third and the fourth ventricles and are rich in fenestrated capillaries with high vascular permeability.[4] Therefore, they function as communication sites between the blood, brain parenchyma, and cerebrospinal fluid, and are thought to be involved in water and energy metabolism, as well as immunomodulation.[1] Among them, the OVLT is a sensory organ, which is an osmotic regulator involved in the release of vasopressin.[6] Vasopressin has been associated with not only blood pressure, but also the generation of endolymphatic hydrops (EH).[7] The patients with Meniere's disease have increased plasma level of vasopressin as well as increased expression of vasopressin type 2 receptor mRNA in endolymphatic sac.[7] In a study of healthy subjects, it was reported that contrast enhancement in the

[1]Department of Radiology, Nagoya University Graduate School of Medicine, 65 Tsurumai-cho, Shouwa-ku, Nagoya, Aichi 466-8550, Japan
[2]Department of Radiology, Aichi Medical University, Aichi, Japan
*Corresponding author, Phone: +81-52-744-2327, Fax: +81-52-744-2335, E-mail: naganawa@med.nagoya-u.ac.jp

Received: June 15, 2017 | Accepted: August 10, 2017

OVLT could be seen in only 34% on 3 Tesla thin slice contrast-enhanced T_1-weighted images.[1]

Image evaluation of EH using MRI in disease conditions such as Meniere's disease has spread widely in clinical practice.[7,8] Previously, intratympanic administration of gadolinium based contrast agents (GBCA) had been utilized.[9,10] However, more recently the method of imaging at 4 h after intravenous administration of a single dose of gadolinium based contrast agent (IV-SD-GBCA) has been widely employed because of the low invasiveness to patients.[11] Heavily T_2-weighted three dimensional-fluid attenuated inversion recovery (3D-FLAIR) (HF) imaging is highly sensitive to low concentrations of contrast medium[12] and is used for endolymphatic hydropic imaging after an IV-SD-GBCA. The GBCA has been reported to distribute not only in the perilymph of the inner ear but also in the cerebrospinal fluid, perivascular space and anterior eye segment by using HF images obtained 4 h after an IV-SD-GBCA.[13]

The objective of this study is to examine gadolinium leakage from the OVLT using HF imaging in healthy subjects, including the time course of enhancement. The results of this study might be useful for understanding the inner ear fluid homeostasis controlled by vasopressin and the pathophysiology of Ménière's disease in the future.

Materials and Methods

The medical ethics committee of our institution approved this study of healthy volunteers and written informed consent was obtained from all participants. Eight male healthy subjects (age 29–53 years old, median: 37 years old) were included in this study. Subjects had no history of ear disease, vertigo, cranial disease, head trauma, renal disease, or heart disease and did not take any daily medications.

Magnetic resonance imaging was performed on a 3T scanner (Verio; Siemens, Erlangen, Germany) using a 32-channel phased array head coil. All subjects underwent heavily T_2-weighted MR cisternography (MRC) for anatomical reference of the fluid space, and HF imaging with an inversion time of 2250 msec according to the clinical protocol of our hospital for evaluating endolymphatic hydrops.[8,13] Briefly, the scan parameters for the MRC were as follows: variable flip angle 3D-turbo spin-echo (sampling perfection with application-optimized contrasts by use of different flip angle evolutions [SPACE]): TR, 4400 msec; TE, 544 msec; initial refocusing 180° flip angle rapidly decreased to a constant 120° flip angle for the turbo spin-echo refocusing echo train; echo train length, 173 with a restore magnetization pulse (fast recovery pulse); matrix size, 322 × 384; 104 axial slices with 1.0-mm-thick; FOV, 15 × 18 cm; generalized autocalibrating partially parallel acquisition (GRAPPA) parallel imaging technique; acceleration factor, 2; number of excitations (NEX), 1.8; and scan time, 3 min. The scan parameters for the HF imaging were similar to those for the MRC except the application of the inversion pulse with an inversion time of 2250 msec; TR, 9000 msec; NEX, 2; and scan time, 7 min. The HF imaging did not utilize a restore pulse. Both the MRC and HF imaging employed an identical FOV, matrix size, and slice thickness to facilitate the comparisons. Sets of MRC and HF images were obtained before and at 0.5, 1.5, 3, 4.5 and 6 h after the IV-SD-GBCA. After the pre-contrast scan, subjects received a single-dose (0.2 ml/kg body weight or 0.1 mmol/kg body weight) with intravenous administration of gadoteridol (Gd-HP-DO3A: ProHance; Eisai, Tokyo, Japan). After the injection of gadoteridol, subjects were permitted to exit the scanner room and rest during the interval between the MR scans without any instructions to restrict behavior. These conditions are basically the same as a previous study.[13]

Image analysis

Images were evaluated qualitatively by two neuroradiologists with more than 20 years' experience and quantitatively by a neuroradiologist with 27 years of experience in the field of clinical MRI. The OVLT is located between the anterior-dorsal aspect of the preoptic recess of the third ventricle, and the prechiasmatic cistern that encloses the preoptic vascular plexus.[14] On mid-sagittal images, the OVLT is located at the anterior wall of the third ventricle between the anterior commissure and the optic chiasma.[1,5] In this study, the OVLT was defined as the horizontal linear or band-like structure located in the anterior wall of the third ventricle at the slice between the slice of the anterior commissure and the slice of the optic chiasm on the axial image. Enhancement was judged as positive if the presumed OVLT and the surrounding cerebral spinal fluid (CSF) had a higher signal on the post-contrast images obtained at the various time points compared to the pre-contrast images.

The signal in the OVLT was measured by positioning a rectangular ROI around the linear or band-like shaped OVLT on the MRC, then copying the ROI to each HF image. The width of the rectangular ROI was 2 mm in the anterior-posterior direction and 3.5 mm in the right-left direction. This rectangular ROI was positioned to contain the linear or band-like OVLT in the center of the ROI and to include the surrounding CSF (Fig. 1). The signal intensity ratio (SIR) was obtained from dividing the signal intensity value of the OVLT by that of the midbrain. A circular ROI with a diameter of 5 mm was set in the midbrain. The averaged SIR values of the eight volunteers were compared among each time point using the univariate repeated measures analysis of variance (ANOVA) with Holm correction for multiple comparisons. For all statistical analyses, we adopted 5% as a significant level. We used software R (version 3.2.3; R Foundation for Statistical, Computing, Vienna, Austria).

The position of enhancement area within the ROI was subjectively classified as "whole ROI", "anterior part of the ROI", "middle part of the ROI", or "posterior part of the ROI" (Fig. 1).

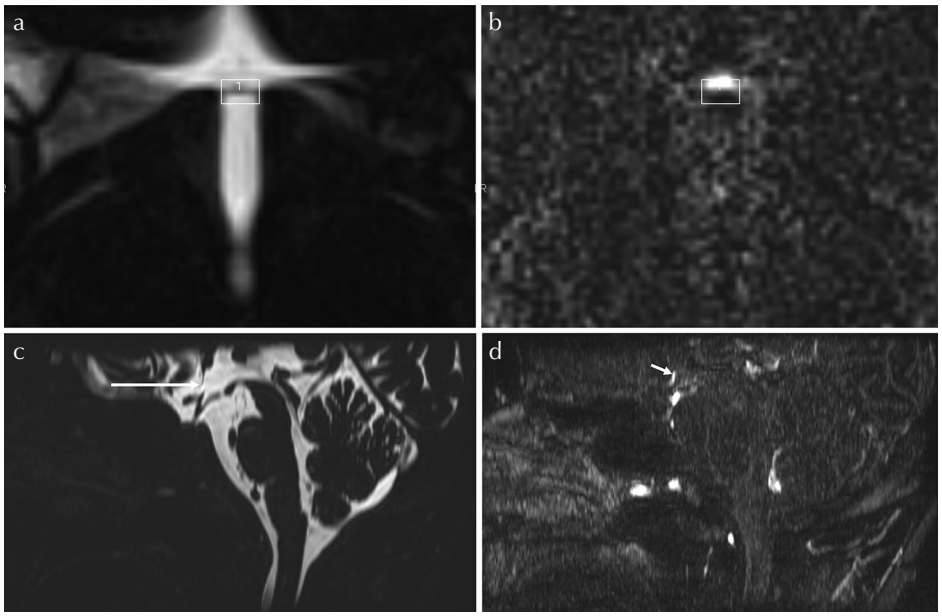

Fig. 1 Example of ROI position. A rectangular ROI is positioned on the MR cisternography (**a**), centered on the band-like organum vasculosus of the lamina terminalis (OVLT). The axial slice of the ROI is positioned in the middle slice level between the anterior commissure and the optic chiasma levels. Then, ROI is copied and pasted onto the corresponding heavily T_2-weighted three dimensional-fluid attenuated inversion recovery (3D-FLAIR) image (**b**). In this volunteer, the position of the enhancement is in the anterior part of the ROI. The mid-sagittal reformatted image of the MR cisternography (**c**) and that of the heavily T_2-weighted 3D-FLAIR obtained 0.5 h after the intravenous single dose administration of gadolinium based contrast agent (IV-SD-GBCA) (**d**) are shown for anatomical orientation. The OVLT is visualized as the slit like low signal structure in the anterior wall of the third ventricle on the MR cisternography (arrow, **c**). Band-like enhancement (short arrow, **d**) just anterior to the OVLT is clearly visualized on the heavily T_2-weighted 3D-FLAIR obtained 0.5 h after the IV-SD-GBCA.

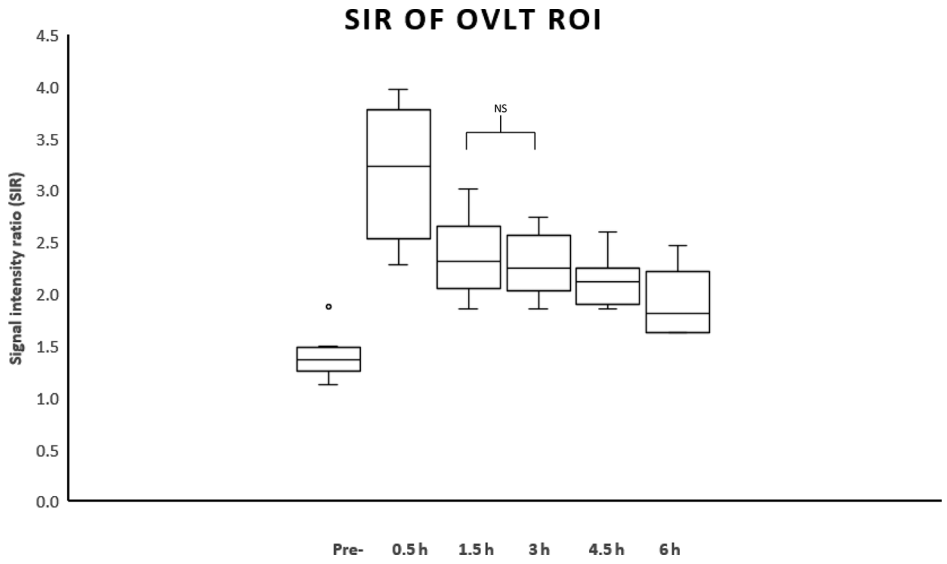

Fig. 2 The signal intensity ratio (SIR) values over time in eight volunteers. The mean SIR at 0.5 h was significantly higher than that at all other time points ($P < 0.05$). The mean SIRs at 0.5, 1.5, 3, 4.5 and 6 h were significantly higher than that at pre-contrast ($P < 0.05$). Only the difference between the mean SIR at 1.5 h and that at 3 h was not significant ($P = 0.0571$, NS). All other pairs showed significant difference. OVLT, Organum vasculosus of the lamina terminalis.

Results

The mean SIR values over time after the IV-SD-GBCA are shown on Fig. 2. The difference between the mean SIR at pre-contrast and those at 0.5, 1.5, 3, 4.5, and 6 h after the IV-SD-GBCA were significant. The differences between the mean SIR at 0.5 h and those at pre-, 1.5, 3, 4.5 and 6 h after the IV-SD-GBCA were significant. The *P*-values of pairwise comparisons are shown in Table 1. Only the difference between the mean SIR at 1.5 h and that at 3 h was not significant ($P = 0.0571$). All other pairs showed significant difference.

The position of the enhancement within the ROI was classified at the time point of 0.5 h because at later time

points, the enhancement was vague with unclear margins. In all subjects, the position of the contrast enhancement was classified as "anterior part of the ROI" by both observers. The degree of enhancement at 0.5 h was classified as "marked" in all subjects by both observers. Marked enhancement was observed only at the 0.5-h time point (Fig. 3).

Discussion

CVOs occupy seven midline locations around the ventricles. They contain specialized ependymal cells known as tanycytes that have an incomplete blood–brain barrier (BBB).[1] The OVLT is covered in a richly fenestrated vascular plexus, which covers glia and network fibers.[3] Fluorescence endoscopy revealed leakage of fluorescence from the ME and OVLT.[15] This technique can be used to visualize important anatomical landmarks during surgical procedures.[16] Enhancement of the OVLT can be seen approximately 20 s after the intravenous administration of fluorescein sodium.[16]

Enhancement on the HF images is usually seen in the fluid space with a long T_2 time. In the present study, the HF images were obtained using a long TR of 9 s and a long inversion time (TI) of 2.25 s. During the long TR and TI, magnetization of the brain tissue is fully recovered, therefore if the GBCA were to leak through an incomplete BBB, the signal of the brain itself would not increase. Furthermore, a very long echo time allows the signal decay in the brain tissue. Thus, the enhancement in the HF images was seen in fluid containing tissue.[11–13,17,18]

Enhancement of the OVLT might be due to the GBCA leakage into the small fluid spaces in the OVLT itself and the CSF space around the surface of the OVTL. The OVLT is reported to have fenestrated capillaries surrounded by extensive perivascular spaces.[4] The position of the enhancement was observed mainly in the CSF just anterior to the OVLT itself. This result indicates that the observed enhancement in the ROI including the OVLT was mainly from leaked GBCA in the CSF anterior to the OVLT. The OVLT is covered by the pia mater on the external surface and with ependyma on the ventricular surface.[4] Therefore, it is reasonable to observe the difference in the leakage of the GBCA between the CSF in the anterior and posterior sides of the OVLT as seen in the present study.

The OVLT receives input from the subforniceal organ, locus ceruleus, and hypothalamic nuclei and projects to the median pre-optic and supra-optic nuclei. It is thought to play a role in controlling the release of vasopressin from the hypothalamic paraventricular and supraoptic nuclei as well as acting as an osmoregulator.[1–3] Vasopressin is reported to be responsible for the generation of EH.[7] It is speculated that the permeability of the OVLT might be also related to EH. This potential relationship warrants further study to reveal the OVLT enhancement in association with the degree of EH.

Table 1. List of *P*-values by the pairwise comparisons among the mean signal intensity ratios (SIRs) at each time points

	Pre	0.5 h	1.5 h	3 h	4.5 h
0.5 h	0.0021				
1.5 h	0.0024	0.0205			
3 h	0.0020	0.0174	0.0571*		
4.5 h	0.0032	0.0092	0.0480	0.0488	
6 h	0.0174	0.0112	0.0112	0.0174	0.0480

The *P* values were adjusted by Holm method, *not significant.

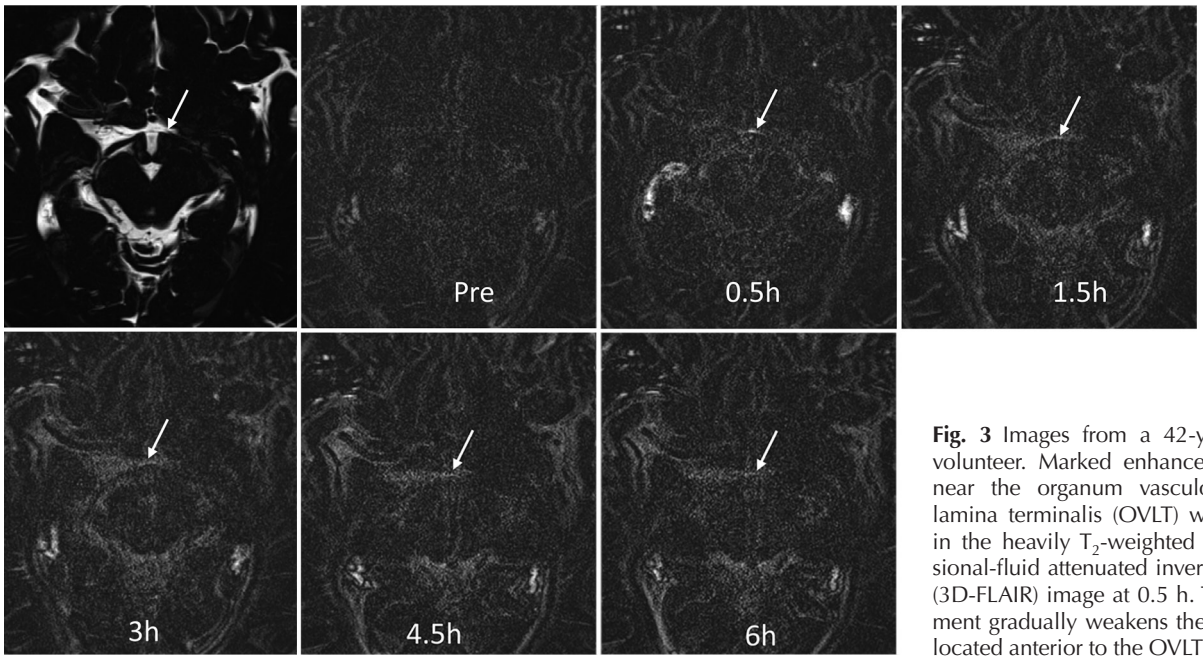

Fig. 3 Images from a 42-year-old male volunteer. Marked enhancement (arrow) near the organum vasculosum of the lamina terminalis (OVLT) was visualized in the heavily T_2-weighted three dimensional-fluid attenuated inversion recovery (3D-FLAIR) image at 0.5 h. The enhancement gradually weakens thereafter and is located anterior to the OVLT itself.

CVOs and the peripheral portions of the cranial nerves are candidates that may be responsible for the permeation of GBCAs to the CSF space. Recently, it was reported that interstitial water infiltration from the capillaries to brain parenchyma might be the main CSF production route, rather than choroid plexus.[19] Some capillaries around the perivascular space might also be a leakage area for GBCAs to the CSF space. Gadolinium deposition in the brain in patients without severe renal insufficiency is receiving great attention from the medical community.[20–22] The pathway for GBCA uptake into the brain is still under discussion. Recently, both linear and macrocyclic type GBCAs were reported to distribute in the CSF space in healthy animals and human subjects without BBB disruption.[13,17,18,23] Permeation of both linear and macrocyclic GBCAs to the perivascular space in normal subjects was also reported.[17,18] The perivascular space is the entry site of the glymphatic system, which is the waste clearance pathway of the brain.[24–31] Therefore the leakage of GBCAs to the CSF space is important to further elucidate this GBCA deposition mechanism.

Enhancement of secretary CVOs and tuber cinereum can be detected constantly even by T_1-weighted images.[5] Among sensory CVOs, not only the OVLT, but also the SFO might relate to the regulation of vasopressin; however, the SFO is a small median structure that lies in the inferior surface of the cerebral fornix and adjacent to the vessels and choroid plexus.[4] Therefore, it is quite difficult to differentiate its enhancement from normally enhancing structures.[1] Thus, we evaluated only the OVLT in the present study.

There are some limitations to this study. We included only a small number of male volunteers. The number of the scan time points was small, especially in the early phase to elucidate the precise point of gadolinium leakage in the OVLT.

Conclusions

Using HF imaging, contrast leakage from the OVLT was readily visualized in all healthy subjects at 0.5 h after an IV-SD-GBCA. Future study is warranted to elucidate the correlation with EH and permeability of the OVLT.

Acknowledgment

This work was supported by JSPS KAKENHI Grant in Aid Numbers JP17H04259, JP16K10312, and JP15K19783.

Conflicts of Interest

All authors do not have any conflicts of interest.

References

1. Horsburgh A, Massoud TF. The circumventricular organs of the brain: conspicuity on clinical 3T MRI and a review of functional anatomy. Surg Radiol Anat 2013; 35:343–349.
2. Ganong WF. Circumventricular organs: definition and role in the regulation of endocrine and autonomic function. Clin Exp Pharmacol Physiol 2000; 27:422–427.
3. Sisó S, Jeffrey M, González L. Sensory circumventricular organs in health and disease. Acta Neuropathol 2010; 120:689–705.
4. Kaur C, Ling EA. The circumventricular organs. Histol Histopathol 2017; 32:879–892.
5. Tsutsumi S, Ono H, Yasumoto Y. The tuber cinereum as a circumventricular organ: an anatomical study using magnetic resonance imaging. Surg Radiol Anat 2017; 39:747–751.
6. Samson WK, Ferguson AV. Exploring the OVLT: insight into a critically important window into the brain. Am J Physiol Regul Integr Comp Physiol 2015; 309:R322–R323.
7. Nakashima T, Pyykkö I, Arroll MA, et al. Meniere's disease. Nat Rev Dis Primers 2016; 2:16028.
8. Naganawa S, Nakashima T. Visualization of endolymphatic hydrops with MR imaging in patients with Ménière's disease and related pathologies: current status of its methods and clinical significance. Jpn J Radiol 2014; 32:191–204.
9. Nakashima T, Naganawa S, Sugiura M, et al. Visualization of endolymphatic hydrops in patients with Meniere's disease. Laryngoscope 2007; 117:415–420.
10. Naganawa S, Satake H, Iwano S, Fukatsu H, Sone M, Nakashima T. Imaging endolymphatic hydrops at 3 tesla using 3D-FLAIR with intratympanic Gd-DTPA administration. Magn Reson Med Sci 2008; 7:85–91.
11. Naganawa S, Yamazaki M, Kawai H, Bokura K, Sone M, Nakashima T. Visualization of endolymphatic hydrops in Ménière's disease with single-dose intravenous gadolinium-based contrast media using heavily T_2-weighted 3D-FLAIR. Magn Reson Med Sci 2010; 9:237–242.
12. Naganawa S, Kawai H, Sone M, Nakashima T. Increased sensitivity to low concentration gadolinium contrast by optimized heavily T2-weighted 3D-FLAIR to visualize endolymphatic space. Magn Reson Med Sci 2010; 9:73–80.
13. Naganawa S, Suzuki K, Yamazaki M, Sakurai Y. Serial scans in healthy volunteers following intravenous administration of gadoteridol: time course of contrast enhancement in various cranial fluid spaces. Magn Reson Med Sci 2014; 13:7–13.
14. Prager-Khoutorsky M, Bourque CW. Anatomical organization of the rat organum vasculosum laminae terminalis. Am J Physiol Regul Integr Comp Physiol 2015; 309:R324–R337.
15. Kubo S, Inui T, Yamazato K. Visualisation of the circumventricular organs by fluorescence endoscopy. J Neurol Neurosurg Psychiatr 2004; 75:180.
16. Longatti P, Basaldella L, Sammartino F, Boaro A, Fiorindi A. Fluorescein-enhanced characterization of additional anatomical landmarks in cerebral ventricular endoscopy. Neurosurgery 2013; 72:855–860.
17. Naganawa S, Nakane T, Kawai H, Taoka T. Lack of contrast enhancement in a giant perivascular space of the basal ganglion on delayed FLAIR images: implications for the glymphatic system. Magn Reson Med Sci 2017; 16: 89–90.
18. Naganawa S, Nakane T, Kawai H, Taoka T. Gd-based contrast enhancement of the perivascular spaces in the basal ganglia. Magn Reson Med Sci 2017; 16:61–65.

19. Orešković D, Radoš M, Klarica M. Cerebrospinal fluid secretion by the choroid plexus? Physiol Rev 2016; 96:1661–1662.
20. Kanda T, Ishii K, Kawaguchi H, Kitajima K, Takenaka D. High signal intensity in the dentate nucleus and globus pallidus on unenhanced T1-weighted MR images: relationship with increasing cumulative dose of a gadolinium-based contrast material. Radiology 2014; 270:834–841.
21. Kanda T, Nakai Y, Aoki S, et al. Contribution of metals to brain MR signal intensity: review articles. Jpn J Radiol 2016; 34:258–266.
22. Kanda T, Nakai Y, Oba H, Toyoda K, Kitajima K, Furui S. Gadolinium deposition in the brain. Magn Reson Imaging 2016; 34:1346–1350.
23. Jost G, Frenzel T, Lohrke J, Lenhard DC, Naganawa S, Pietsch H. Penetration and distribution of gadolinium-based contrast agents into the cerebrospinal fluid in healthy rats: a potential pathway of entry into the brain tissue. Eur Radiol 2017; 27:2877–2885.
24. Iliff JJ, Lee H, Yu M, et al. Brain-wide pathway for waste clearance captured by contrast-enhanced MRI. J Clin Invest 2013; 123:1299–1309.
25. Iliff JJ, Nedergaard M. Is there a cerebral lymphatic system? Stroke 2013; 44:S93–S95.
26. Iliff JJ, Wang M, Zeppenfeld DM, et al. Cerebral arterial pulsation drives paravascular CSF-interstitial fluid exchange in the murine brain. J Neurosci 2013; 33:18190–18199.
27. Yang L, Kress BT, Weber HJ, et al. Evaluating glymphatic pathway function utilizing clinically relevant intrathecal infusion of CSF tracer. J Transl Med 2013; 11:107.
28. Iliff JJ, Chen MJ, Plog BA, et al. Impairment of glymphatic pathway function promotes tau pathology after traumatic brain injury. J Neurosci 2014; 34:16180–16193.
29. Kress BT, Iliff JJ, Xia M, et al. Impairment of paravascular clearance pathways in the aging brain. Ann Neurol 2014; 76:845–861.
30. Simon MJ, Iliff JJ. Regulation of cerebrospinal fluid (CSF) flow in neurodegenerative, neurovascular and neuroinflammatory disease. Biochim Biophys Acta 2016; 1862: 442–451.
31. Zeppenfeld DM, Simon M, Haswell JD, et al. Association of perivascular localization of aquaporin-4 with cognition and alzheimer disease in aging brains. JAMA Neurol 2017; 74:91–99.